Research Article Vol. 41, No. 5 / May 2024 / Journal of the Optical Society of America B 1217

Journal of the Optical Society of America B

OPTICAL PHYSICS

Spectroscopic study of the $4f^7 6s^2 {}^8S^\circ_{7/2} - 4f^7({}^8S^\circ)6s6p({}^1P^\circ)\,{}^8P_{5/2,7/2}$ transitions in neutral europium-151 and europium-153: absolute frequency and hyperfine structure

C. Maruko,[1,2,†] N. N. Çölmek,[1,†] M. T. Herd,[3] K. J. Ahrendsen,[1] B. Cabrales,[1] G. Cannon,[3] E. Davis,[1] X. Y. Guo,[1] T. Karani,[1] A. Wallace,[1] K. Wisnauckas,[1] and W. D. Williams[1,*]

[1]Department of Physics, Smith College, 44 College Lane, Northampton, Massachusetts 01063, USA
[2]Current address: JILA, NIST, and Department of Physics, University of Colorado, 440 UCB, Boulder, Colorado 80309, USA
[3]Department of Biological and Physical Sciences, Assumption University, Worcester, Massachusetts 01609, USA
[†]These authors contributed equally to this work.
*wraven@smith.edu

Received 7 February 2024; revised 1 April 2024; accepted 12 April 2024; posted 12 April 2024; published 25 April 2024

We report on spectroscopic measurements on the $4f^7 6s^2\,{}^8S^\circ_{7/2} - 4f^7({}^8S^\circ)6s6p({}^1P^\circ)\,{}^8P_{5/2,7/2}$ transitions at 466.32 nm and 462.85 nm, respectively, in neutral europium-151 and europium-153. The center of gravity frequencies for the 151 and 153 isotopes for both transitions are reported for the first time using saturated absorption spectroscopy. For the $6s6p({}^1P^\circ)\,{}^8P_{5/2}$ state, the center of gravity frequencies were found to be 642,894,493.3(4) MHz and 642,891,693.3(9) MHz for the 151 and 153 isotopes, respectively. The hyperfine constants for the upper state were found to be $A(151) = -157.01(3)$ MHz, $B(151) = 74.5(4)$ MHz and $A(153) = -69.43(14)$ MHz, $B(153) = 191.0(26)$ MHz. These hyperfine values are all consistent with previously published results except for $B(151)$ that has a small discrepancy. The isotope shift was found to be 2799.54(20) MHz, a small discrepancy with previously published results. For the $6s6p({}^1P^\circ)\,{}^8P_{7/2}$ state, the center of gravity frequencies were found to be 647,708,930.6(6) MHz and 647,705,958.4(26) MHz for the 151 and 153 isotopes, respectively. The hyperfine constants for the upper state were found to be $A(151) = -218.66(4)$ MHz, $B(151) = -293.4(8)$ MHz and $A(153) = -97.15(13)$ MHz, $B(153) = -750(3)$ MHz. These values are all consistent with previously published results except for $A(151)$ that has a small discrepancy. The isotope shift was found to be 2972.8(5) MHz, a small discrepancy with previously measured results.

https://doi.org/10.1364/JOSAB.521181

1. INTRODUCTION

In the last decade, there has been an increased focus on the neutral europium atom, a lanthanide element with 63 protons and two stable isotopes. The absolute transition frequency for both stable isotopes between the ground state and the $4f^7({}^8S^\circ)6s6p({}^1P^\circ)\,{}^8P_{9/2}$ state, historically known as the $y\,{}^8P_{9/2}$ state, was recently measured to sub-MHz precision [1], and the branching ratios from the $y\,{}^8P_{9/2}$ state were also measured [2]. A magneto-optical trap of ultracold europium was created by Kozuma *et al.* [3,4] and used to populate lower lying metastable states to study one-body losses in magnetically trapped europium [5]. A europium Bose–Einstein condensate (BEC) was successfully created in 2022 [6], and a proposal to create a dual species rubidium and europium BEC was recently published [7]. Despite the interest in europium, there is a dearth of high precision (sub-MHz) measurements.

Europium has two stable isotopes, europium-151 (47.8% natural abundance) and europium-153 (52.2%). Both isotopes have the same nuclear spin of $I = 5/2$. The isotope shift and hyperfine constants for a large variety of states have been measured. For a recent compilation of these measurements from 2020, see reference [8].

The subjects of this paper are the $4f^7({}^8S^\circ)6s6p({}^1P^\circ)\,{}^8P_{5/2}$ state, historically known as the $y\,{}^8P_{5/2}$ state, and the $4f^7({}^8S^\circ)6s6p({}^1P^\circ)\,{}^8P_{7/2}$ state, historically known as the $y\,{}^8P_{7/2}$ state. The transitions were first measured by Russell and King in 1939 using an arc lamp [9] and most recently measured in 1983 by Smith and Tomkins [10]. However, these measurements had unresolved hyperfine structure and overlapping spectrums, so the reported values of 21, 444.60(1) cm^{-1}

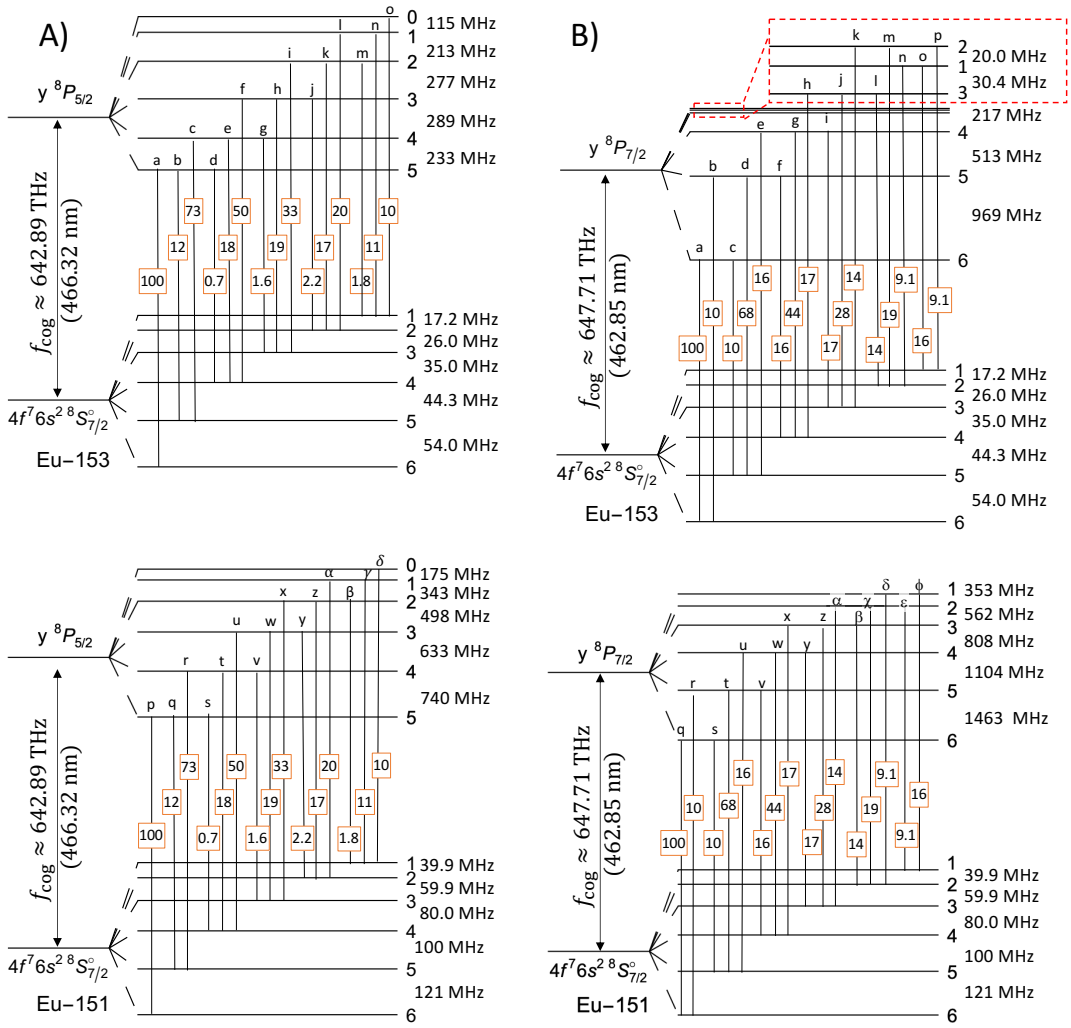

Fig. 1. Simplified Grotrian diagrams for europium-153 (top) and 151 (bottom) for transitions from the ground state to the (A) $y\ ^8P_{5/2}$ state and (B) $y\ ^8P_{7/2}$ state. The boxed values represent the relative intensities of the allowed transitions, normalized to the strongest transition. The left of each diagram shows the center of gravity transition frequency.

(642, 892, 900(300) MHz) for the $y\ ^8P_{5/2}$ state and 21, 605.18(1) cm^{-1}(647, 707, 000(300) MHz) for the $y\ ^8P_{7/2}$ state were limited by Doppler broadening which resulted in a spectrum width of 0.2 cm^{-1}(6000 MHz). Thus, the center of gravity for these transitions has yet to be measured to high precision for each isotope. Simplified Grotrian diagrams for the two stable isotopes are shown in Fig. 1. The formula below gives relative intensities of the hyperfine transitions:

$$I_r = (2F+1)(2F'+1)\begin{Bmatrix} J & I & F \\ F' & 1 & J' \end{Bmatrix}^2, \tag{1}$$

where the J and F are the total electronic angular momentum and total atomic angular momentum for the ground state, and J' and F' are the quantum numbers for either the $y\ ^8P_{5/2}$ or $y\ ^8P_{7/2}$ excited states. We normalized the intensities by referencing the largest intensity transition, which was $F = 6 \rightarrow F' = 6$ for the $y\ ^8P_{7/2}$ state and $F = 6 \rightarrow F' = 5$ for the $y\ ^8P_{5/2}$ state. Figure 1 displays the normalized intensities of the transitions within boxes. Because quantum interference effects from the many overlapping spectral features likely modified these anticipated amplitude ratios [11], we used them as an aid in identifying spectral features, not as a fixed fit parameter.

In the absence of nuclear spin, there would be a single lower state and a single upper state; see Fig. 1. Since both studied isotopes have nuclear spin, there is a splitting of the center of gravity given by the hyperfine splitting formula,

$$\frac{1}{2}AK + B\frac{(3/2)K(K+1) - 2I(I+1)J(J+1)}{2I(2I-1)2J(2J-1)}, \tag{2}$$

where $K = F(F+1) - I(I+1) - J(J+1)$, A is the magnetic dipole constant, and B is the electric quadrupole constant. The higher order terms for Eq. (2) were not included since they are beyond the scope of our precision. For the ground state, the most precise value for the hyperfine constants were measured by Sanders and Woodgate with values $A(151) = -20.0523(2)$ MHz, $B(151) = -0.7012(35)$ MHz, $A(153) = -8.8532(2)$ MHz, and $B(153) = -1.7852(35)$ MHz [12]. Before this work, the best values for the excited state hyperfine constants were measured by Zaal *et al.* with values $A(151) = -157.2(3)$ MHz, $B(151) = 78(3)$ MHz,

$A(153) = -69.2(3)$ MHz, and $B(153) = 192(3)$ MHz for the $y\,^8P_{5/2}$ state and $A(151) = -219.1(2)$ MHz, $B(151) = -295(3)$ MHz, $A(153) = -97.0(4)$ MHz, and $B(153) = -753(7)$ MHz for the $y\,^8P_{7/2}$ state [13].

We used saturated absorption spectroscopy to measure for the first time the center of gravity absolute transition frequencies from the ground state to the $y\,^8P_{5/2}$ and $y\,^8P_{7/2}$ states. Combined with previously published results [1], all transitions from the ground state to the $y\,^8P_J$ states have been measured to sub-MHz precision. We also measured the hyperfine constants for the two excited states, improving the precision of some values by an order of magnitude, and the isotope shifts, both improving the precision and correcting a slight discrepancy with previously reported values [13]. The paper is organized as follows: Section 2 contains a summary of the experimental setup, Section 3 presents our findings and discusses systematic effects, and Section 4 concludes with an overview of results and outlines methods to improve the precision of future measurements.

2. EXPERIMENTAL SETUP

Figure 2 shows a simplified experimental setup for this work. Details of the experimental setup can be found in reference [1]. Briefly, a titanium sapphire laser (M Squared SolsTiS) is used to produce infrared light that is half the frequency needed for the spectroscopic studies. This light is sent to a double pass AOM (Brimrose GPM-800-200) setup [14] before being locked to a mode of the frequency comb spectrum. An FPGA based digital locking system (TOPTICA DigiLock 110) is used providing fast and slow feedback to two piezos, both actuating the laser's cavity, with different bandwidths (~ 50 Hz and ~ 30 kHz). Once stabilized to the comb, the frequency of the light leaving the titanium sapphire laser is

$$f_{IR} = n f_{rep} + f_{beat} - 2 f_{AOM}, \tag{3}$$

where n is the frequency comb order, $f_{rep} = 80$ MHz is the repetition rate of the comb, $f_{beat} = +20$ MHz is the beat frequency between the laser and the nearest comb order, and f_{AOM} is the frequency driving the double pass AOM. With this setup, the frequency of the laser can be scanned ≈ 650 MHz with uncertainty better than 1.5 kHz.

The infrared light is then frequency doubled before it is sent to a saturated absorption setup. The frequency of the blue light can be scanned with respect to the frequency comb for a total scan range of up to ≈ 1300 MHz with uncertainty better than 3 kHz. The pump light is amplitude modulated using the positive first order of an AOM (ISOMET M1201-SF40-1.7) operating at 40 MHz, which shifts the spectrum lower by 20 MHz. A photodetector (Thorlabs PDA36A) monitors the transmission of the probe light through the europium hollow cathode lamp. The spectral signal from the photodetector is isolated by a lock-in amplifier (Stanford Research Systems SR830) using the 27.13 kHz AOM modulation frequency and then recorded by a computer.

The gaseous europium is created by a home-built, see-through, hollow cathode lamp (HCL) [1,15]. The HCL is backfilled with argon pressures ranging between 280 mTorr and 580 mTorr and driven by a power supply (KEPCO BOP 500 M) with currents ranging from -3 mA to -8 mA and voltages ranging from -150 V to -350 V. The power supply can be run in constant current or constant voltage mode. Constant voltage mode is used to investigate energy level shifts due to the applied

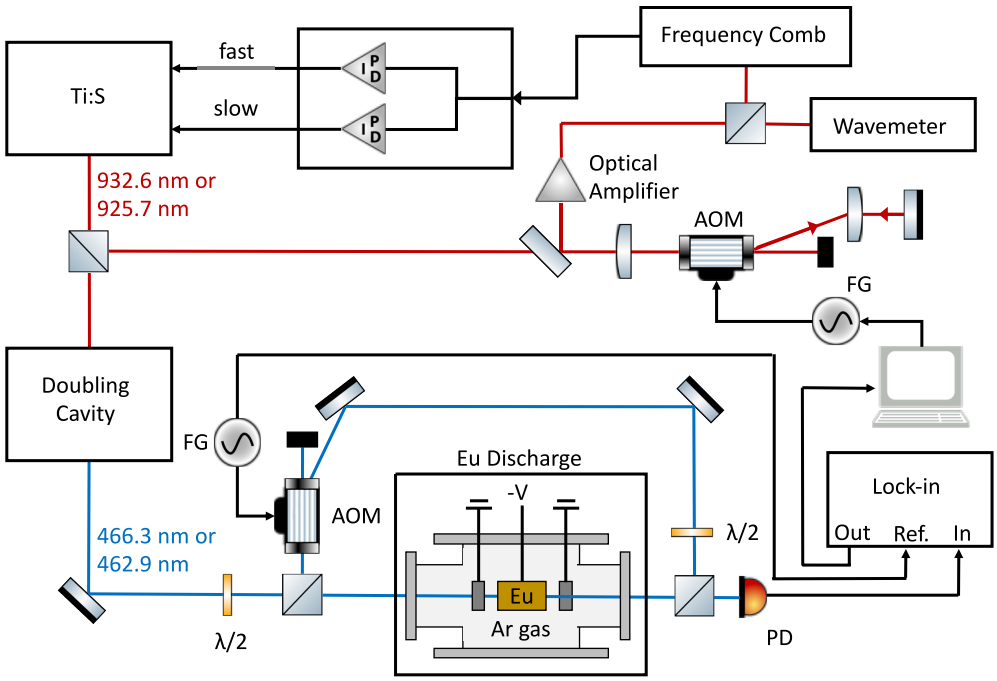

Fig. 2. Simplified experimental setup. The upper half of the diagram shows a double-pass AOM setup for the scanning and stabilization of laser. The lower half of the diagram shows a saturated absorption setup and europium discharge used for spectroscopy. PD: photodetector, AOM: acousto-optic modulator, FG: function generator.

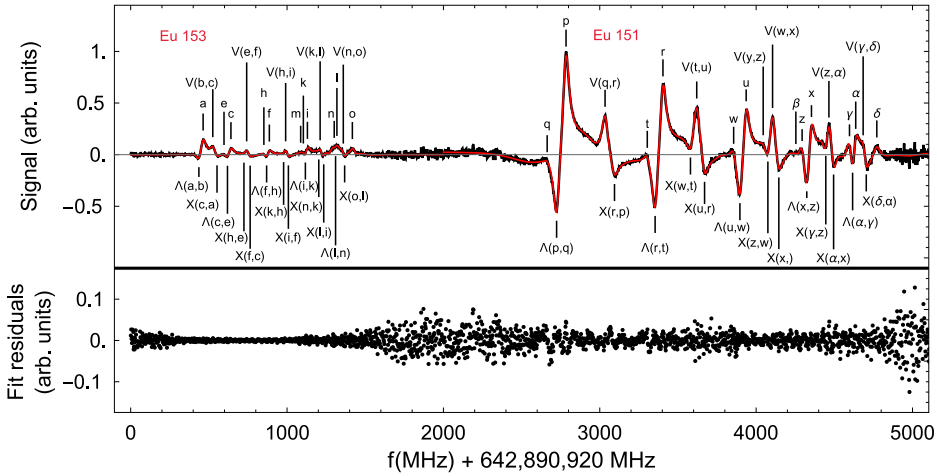

Fig. 3. An example of a fitted spectrum for the $4f^7 6s^2\,{}^8S^o_{7/2} - y\,{}^8P_{5/2}$ transition in neutral europium-153 (spectral features with $f < 2000$ MHz) and europium-151 (spectral features with $f > 2000$ MHz) near 466.32 nm. The data are in black; the fit is in red. Included are indicators for which transition or crossover is responsible for the spectral feature based on the labels from Fig. 1. Below the spectrum is a plot of the fit residuals. The vertical scale for the residuals is magnified by a factor of 4 for visibility.

external voltage, but constant current mode was used while studying the other systematic effects.

3. RESULTS

Due to a limited scan range of the double pass AOM, data are collected in frequency scans of 1320 MHz. The spectra (see Figs. 3 and 4) are approximately 5 GHz and 6.5 GHz wide, requiring multiple regions of data collection. Each region overlaps with the proximate by 40 MHz. The data are then stitched together prior to fitting.

As can be seen in Figs. 3 and 4, the spectra from the two isotopes are well separated. The lower frequency ranges of both spectra are due to transitions and crossovers from the europium-153 isotope while the features in the higher frequency range are due to transitions and crossovers in europium-151. The large number of hyperfine states and transitions with overlapping Doppler profiles results in many crossover features. All three types of crossovers, V, Λ, and X, were considered during analysis. V crossovers are created when the pump and probe beam try to excite the same atoms from the same ground state to different excited states and tend to be positive amplitude spectral features. Λ and X crossovers, which tend to be negative amplitude spectral features, occur when the pump beam excites an atom with a particular velocity such that upon decay to a different ground state that atom has the correct velocity to be excited by the probe beam. In all, each isotope has 15 (16) real transitions and up to 62 (68) crossovers for the $4f^7 6s^2\,{}^8S^o_{7/2} - y\,{}^8P_{5/2}$ ($y\,{}^8P_{7/2}$) transition, for a total of 77 (84) possible spectral features to fit. However, not all transitions and possible crossovers were seen in the spectrum; see Section 3.A.

The experiment contains several systematics that may cause a shift in the measured frequency of the transition. We tested the pressure of the argon gas, the voltage driving the discharge, and the laser power. We systematically varied each of these parameters to quantify their effect on our measured transition frequency. Spectra were taken at argon pressures of 279.1 mTorr, 328.7 mTorr, 411.5 mTorr, 494.3 mTorr, and 577.0 mTorr. Probe (pump) saturation parameters of 0.2 (1), 0.4 (2), 0.6 (3), 0.8 (4), and 1 (5) were used to investigate the effect of laser power. For the voltage systematic, the power supply was run in constant voltage mode with voltages of −225 V, −250 V, −275 V, −300 V, and −325 V. While checking one systematic the other values were held constant: 328.7 mTorr for pressure, −7 mA for current driving the discharge, and 0.6 (3) for the probe (diffracted pump beam) saturation parameters. Eight scans were collected for each of the 15 systematic values for a total of 120 scans.

A. Data Analysis

Due to the large number of possible spectral features and the complexity of the spectrum, we use the following procedure to select features and avoid overfitting. To begin, the previously measured hyperfine constants and isotope shifts [13] were used to identify an isolated spectral feature or nearly isolated spectral features. For the transition to the $y\,{}^8P_{5/2}$ state, the largest lowest frequency features [the real transition labeled a and the Λ crossover labeled $\Lambda(a, b)$] were used for initial placement of possible spectral features for europium-153. Likewise, the real transition p and the Λ crossover $\Lambda(p, q)$ were used for europium-151. For the transition to the $y\,{}^8P_{7/2}$ state, the real transition a and the Λ crossover $\Lambda(a, c)$ were used for europium-153. For europium-151 the real transition q and the Λ crossover $\Lambda(q, s)$ were used; see Figs. 3 and 4.

Using Eq. (2) and the previously measured hyperfine constants [12,13], an initial guess for all possible spectral features and center of gravity frequencies can be made with reference to the above-mentioned isolated spectral features. In these predictions, we saw the value drifting to higher frequencies compared to the observed spectral features, indicating a possible small frequency calibration error in Ref. [13].

Once we estimated the initial positions, we analyzed the spectra to determine which specific spectral features were present.

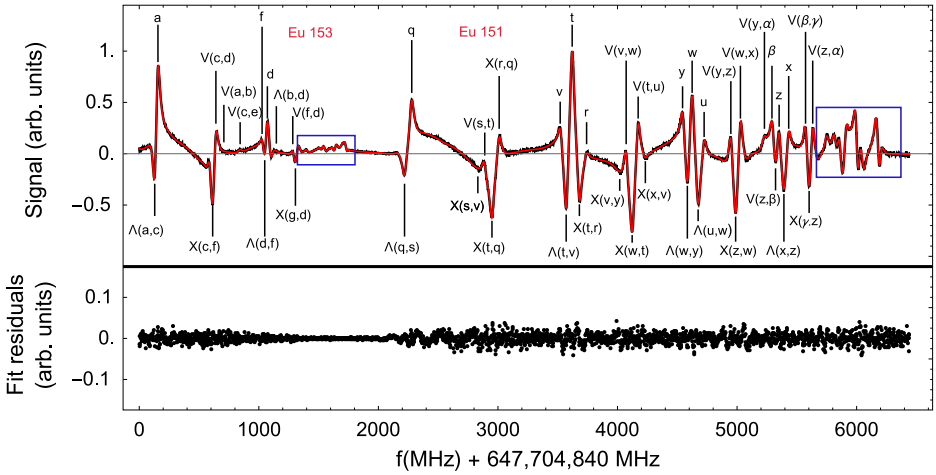

Fig. 4. An example of a fitted spectrum for the $4f^7 6s^2\,{}^8S^\circ_{7/2} - y\,{}^8P_{7/2}$ transition in neutral europium-153 (spectral features with $f < 2000$ MHz) and europium-151 (spectral features with $f > 2000$ MHz) near 462.85 nm. The data are in black; the fit is in red. Included are indicators for which transition or crossover is responsible for the spectral feature based on the labels from Fig. 1. Due to the density of spectral features inside the regions indicated by the blue boxes, the transitions and crossovers labels in those regions are not listed. Below the spectrum is a plot of the fit residuals. The vertical scale for the residuals is magnified by a factor of 4 for visibility.

Table 1. Number of Spectral Features Used to Fit the Data

Upper State	$y\,{}^8P_{5/2}$		$y\,{}^8P_{7/2}$	
Isotope	151	153	151	153
Total possible transitions	77		84	
Transitions used in fit	31	29	47	27
Transitions unique to isotope	2	0	21	1

Reasons why a possible spectral feature is absent include weak relative intensities, a feature that would require a large Doppler shift, or an X crossover feature resulting from a single velocity class. For much of the spectrum, a positive amplitude spectral feature is near a negative amplitude spectral feature giving the appearance of a derivative "S" shaped signal. It should be emphasized that there are no derivative features in the spectrum; the spectrum is produced using amplitude modulation.

Table 1 lists the number of spectral features identified as present and used in the final fitting for each spectrum. It should be noted that for the $y\,{}^8P_{7/2}$ state there could be more contributions for europium-153 at the larger frequency range (near 1700 MHz in Fig. 4), but the closely spaced hyperfine levels (see Fig. 1) did not require additional features to be included in the fit function. Including additional features in this region predictably results in larger off diagonal elements in the correlation matrix for the fitted amplitude parameters without affecting the fitted values or uncertainties for the hyperfine constants or center of gravity frequency.

Once the possible transitions and crossovers were selected, the spectra were fit using Mathematica's NonlinearModelFit function, assuming the ground state hyperfine constants were known, and using the previously measured excited state hyperfine constants [13] as initial guesses. No attempt was made to correct for instrument broadening, so spectral widths will include the 300 kHz shape of the laser.

Gaussian pedestals were observed on several of the spectral features. Referring to Fig. 4, this is most evident on the features a near 150 MHz and q near 2250 MHz. The background pedestals got smaller as the argon pressure was reduced, which indicates the presence of velocity changing collisions [18]. Pedestals were included in the fit function for spectral features which clearly exhibited this structure. The spectrum was fit to a sum of Lorentzian functions and Gaussian functions:

$$s(f) = \sum_i \frac{A_{L,i}}{1 + \frac{4(f-f_i)^2}{\gamma^2}} + A_{G,i} e^{-\frac{(f-f_i)^2}{2\sigma^2}},$$

$$f_i = n_1 A_{gs} + n_2 B_{gs} + n_3 A_{es} + n_4 B_{es} + f_{\mathrm{cog}},$$

where n_1, n_2, n_3, and n_4 are fractions determined from Eq. (2), A_{gs} and B_{gs} are the hyperfine constants for the ground state for a particular isotope, A_{es} and B_{es} are the hyperfine constants for either the $y\,{}^8P_{5/2}$ or $y\,{}^8P_{7/2}$ state for a particular isotope, $A_{L,i}$ is the amplitude of a spectral feature, and $A_{G,i}$ is the amplitude of the Gaussian pedestal, which is only included if it is visible in the spectrum. Due to likely quantum interference effects from the many overlapping spectral features [11], the amplitudes for all spectral features are free parameters. The full width half maxima, γ, is assumed to be the same for all spectral features. The width of the Gaussian pedestals, σ, is assumed to be the same for all features exhibiting that characteristic; allowing variable pedestal widths for each spectral feature did not change the final results for the hyperfine constants or center of gravity frequencies. The full width half maximum of spectral features (see Fig. 5 for an example using the $4f^7 6s^2\,{}^8S^\circ_{7/2} - y\,{}^8P_{5/2}$ transition in europium-151) decreased linearly with background pressure.

Figures 3 and 4 show examples of a fitted spectrum with residuals. All 120 scans were fit individually to extract the hyperfine constants and center of gravity frequencies for both isotopes with uncertainties. During data collection, alternating scans of linearly increasing laser frequency (scan up) and linearly decreasing laser frequency (scan down) were taken to check for hysteresis effects. For the center of gravity frequencies, a small hysteresis effect of less than 1 MHz was seen between scan up

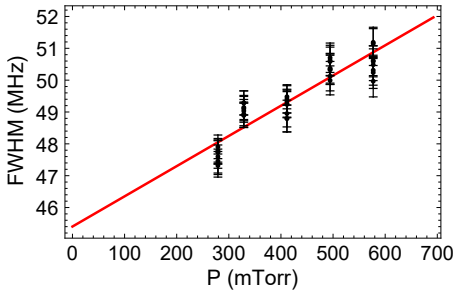

Fig. 5. The fitted full width half maximum for the spectral features in the $4f^7 6s^2\,{}^8S^o_{7/2} - y\,{}^8P_{5/2}$ transition for europium-151. The natural linewidth of this transition is 24.2 MHz [16,17].

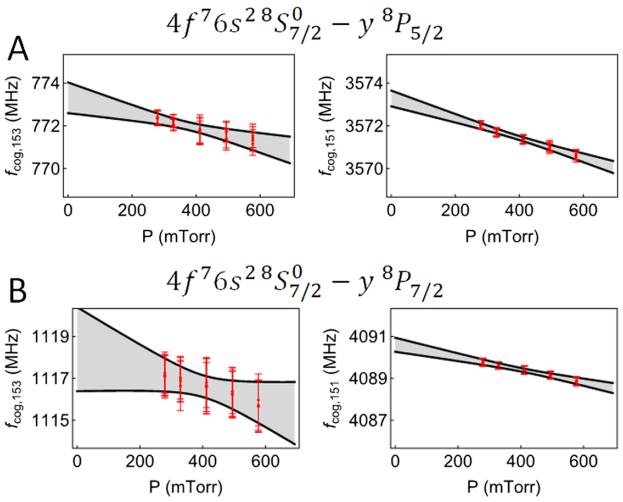

Fig. 6. Pressure shift for the center of gravity frequency of europium-153 and europium-151 for the transitions from the ground state to (A) the $y\,{}^8P_{5/2}$ state and (B) the $y\,{}^8P_{7/2}$ state. The vertical axis on the pressure shift plots are with respect to the offsets given in Figs. 3 and 4.

and scan down. To account for this effect, the center of gravity frequency result for a scan up is averaged with the following scan down result. The uncertainty of this average is taken to be the larger of the two individual fit uncertainties.

As mentioned above, the argon discharge pressure, voltage driving the discharge, and laser power were all varied to look for systematic shifts. A small pressure shift was seen in the center of gravity frequencies for both studied transitions. The difference between the center of gravity frequencies for the two stable isotopes showed no statistical pressure dependence indicating both isotopes experienced a similar shift with background pressure. Figure 6 shows the results of the pressure systematic study. Mathematica's NonlinearModelFit function was used to linearly extrapolate the center of gravity frequencies, with uncertainties, to 0 pressure. All fitted slopes were consistent with each other. For the transition to the $y\,{}^8P_{5/2}$ state, the fitted slopes were −4.6(10) kHz/mTorr for europium-151 and −3.5(20) kHz/mTorr for europium-153. For the transition to the $y\,{}^8P_{7/2}$ state, the fitted slopes were −3.0(8) kHz/mTorr for europium-151 and −4(5) kHz/mTorr for europium-153. Each graph in Fig. 6 has the same vertical scale for visual comparison of the slopes. No dependence on discharge voltage or laser power was seen within our experimental uncertainty.

The isotope shift for both transitions was determined using all scans. The shift was statistically independent of experimental parameters. The values given in Table 2 are the average value of all isotope shift measurements with uncertainty given by the standard deviation.

Table 2 shows the final results of this spectral analysis. The uncertainties for the hyperfine constants were determined by analyzing histograms from all 120 fits. The histograms were all nearly Gaussian. To avoid underestimating the uncertainty due to having nonperfect Gaussian distributions, the standard deviation of the fits were used instead of the standard deviation of the mean. Contributions to the uncertainties for the center of gravity frequencies include the 0 pressure extrapolations, spread of fit values for both laser saturation and discharge voltage (uncertainty in stating these parameters had 0 slope), pump/probe overlap, and uncertainty of the frequency of the laser. The pump and probe beams overlap for about 1 m resulting in a pump/probe parallel uncertainty of 0.5 mRad, which leads to an absolute frequency uncertainty of less than 100 kHz [19]. The uncertainty of the laser frequency is less than 3 kHz. These uncertainties are added in quadrature to give the final uncertainties of the center of gravity frequencies given in Table 2. All of the uncertainties are summarized in Table 3.

The center of gravity for the two stable isotopes agrees well with the Doppler broadened spectra obtained by Smith and Tomkins, whose Doppler broadened spectrum had a center value of 652, 387, 360 ± 600 MHz and a width of 6000 MHz [10]. There is a slight disagreement with previously published results for europium-151 for the magnetic dipole hyperfine constant of the $y\,{}^8P_{5/2}$ state and the electric quadrupole hyperfine constant for the $y\,{}^8P_{7/2}$ state. There was also a small discrepancy in the isotope shift for both transitions [13].

Table 2. Final Results for the Spectral Analysis of the $y\,{}^8P_{5/2}$ and $y\,{}^8P_{7/2}$ States

	$y\,{}^8P_{5/2}$		$y\,{}^8P_{7/2}$	
Units: MHz	**This Work**	**From Ref. [13]**	**This Work**	**From Ref. [13]**
A(151)	−157.01(3)	−157.2(3)	−218.66(4)	−219.1(2)
B(151)	74.5(4)	78(3)	−293.4(8)	−295(3)
A(153)	−69.43(14)	−69.2(3)	−97.15(13)	−97.0(4)
B(153)	191.0(26)	192(3)	−750(3)	−753(7)
f_{cog}(151)	642,894,493.3(4)		647,708,930.6(6)	
f_{cog}(153)	642,891,693.3(9)		647,705,958.4(26)	
Isotope Shift	2799.54(20)	2804(2)	2972.8(5)	2977(2)

Table 3. Error Budget for the Center of Gravity Frequencies

	$y\,^8P_{5/2}$		$y\,^8P_{7/2}$	
Units: kHz	**Eu-151**	**Eu-153**	**Eu-151**	**Eu-153**
Pressure Extrapolation	300	800	240	2100
RF Discharge Voltage	200	150	500	1300
Laser Power	150	350	300	900
Pump/probe parallelism	100	100	100	100
Laser frequency	3	3	3	3
Overall (quadrature sum)	400	900	600	2600

4. CONCLUSION AND FUTURE WORK

This paper reports the first measurements of the center of gravity frequencies for $4f^7 6s^2\,{}^8S^\circ_{7/2} - 4f^7(^8S^\circ)6s\,6p(^1P^\circ)\,{}^8P_{5/2}$ and $4f^7 6s^2\,{}^8S^\circ_{7/2} - 4f^7(^8S^\circ)6s\,6p(^1P^\circ)\,{}^8P_{7/2}$ transitions in neutral europium-151 and europium-153. We found a small discrepancy in the hyperfine constants for europium-151 for the $y\,^8P_{5/2}$ B constant and $y\,^8P_{7/2}$ A constant. There is also a discrepancy in the isotope shift measurement for both isotopes. Otherwise, our results are in good agreement with previously published results. Combined with previously published results [1], all transitions from the ground state to the $y\,^8P_J$ states have been measured to sub-MHz precision.

Further reduction in the number of crossover features, and thus a possible improvement in the statistical results, can be obtained by either performing crossover-free saturated absorption spectroscopy [20], by cooling the hollow cathode lamp to reduce the Doppler width of the individual transitions, by performing the spectroscopy on a well collimated atomic beam, or by performing spectroscopy on laser cooled and trapped europium atoms [3,4,6].

Funding. Directorate for Mathematical and Physical Sciences (PHY-2110311).

Acknowledgment. The authors would like to thank Ibrahim Sulai of Bucknell University for sharing his design for the hollow cathode lamp and for discussions on fitting, and Dale Renfrow from the Smith College Center for Design and Fabrication for building the lamp. This paper is the result of a course-based research program designed for first-year college students (freshmen). The authors would like to thank the Smith College Office of the Provost and Dean of Faculty for personnel support to make this class possible. The authors would also like to thank Timothy Malacarne of Nevada State University and Patricia DiBartolo of Smith College for pedagogical discussions when designing this class.

Disclosures. The authors declare no conflicts of interest.

Data availability. Data underlying the results presented in this paper are not publicly available at this time but may be obtained from the authors upon request.

REFERENCES

1. M. T. Herd, C. Maruko, M. M. Herzog, *et al.*, "Spectroscopic study of the $4f^7 6s^2 {}^8S_{7/2}^\circ$ – $4f^7(^8S^\circ)$ $6s6p(^1P^\circ)$ $^8P_{9/2}$ transition in neutral europium-151 and europium-153: absolute frequency and hyperfine structure," J. Opt. Soc. Am. B **39**, 2596–2602 (2022).
2. Y. Miyazawa, R. Inoue, K. Nishida, *et al.*, "Measuring the branching ratios from the $y^8P_{9/2}$ state to metastable states in europium," Optics Communications **392**, 171–174 (2017).
3. R. Inoue, Y. Miyazawa, and M. Kozuma, "Magneto-optical trapping of optically pumped metastable europium," Phys. Rev. A **97**, 061607 (2018).
4. Y. Miyazawa, R. Inoue, H. Matsui, *et al.*, "Narrow-line magneto-optical trap for europium," Phys. Rev. A **103**, 053122 (2021).
5. H. Matsui, Y. Miyazawa, R. Inoue, *et al.*, "Understanding one-body losses in magnetically trapped metastable europium atoms," Opt. Commun. **502**, 127408 (2022).
6. Y. Miyazawa, R. Inoue, H. Matsui, *et al.*, "Bose-Einstein condensation of Europium," Phys. Rev. Lett. **129**, 223401 (2022).
7. S. Li, U. N. Le, and H. Saito, "Long-lifetime supersolid in a two-component dipolar Bose-Einstein condensate," Phys. Rev. A **105**, L061302 (2022).
8. B. Furmann, M. Chomski, M. Suski, *et al.*, "Investigations of the hyperfine structure and isotope shifts in the even-parity level system of atomic Europium," J. Quant. Spectrosc. Radiat. Transfer **251**, 107070 (2020).
9. H. N. Russell and A. S. King, "The arc spectrum of Europium," Astrophys. J. **90**, 155 (1939).
10. G. Smith and F. Tomkins, "Absorption spectroscopy of laser excited europium vapour," Proc. R. Soc. London A **387**, 389–406 (1983).
11. R. Brown, S. Wu, J. Porto, *et al.*, "Light polarization and quantum interference effects in unresolvable atomic lines: application to a precise measurement of the ^{6,7}Li D_2 lines," Phys. Rev. A **87**, 032504 (2013).
12. P. G. H. Sandars and G. K. Woodgate, "Hyperfine structure in the ground state of the stable isotopes of Europium," Proc. R. Soc. London A **257**, 269–276 (1960).
13. G. J. Zaal, W. T. Hogervorst, E. R. Eliel, *et al.*, "A high resolution study of the transitions $4f^7 6s^2 \rightarrow 4f^7 6s6p$ in the Eu I-spectrum," Z. Phys. A **290**, 339–344 (1979).
14. E. A. Donley, T. P. Heavner, F. Levi, *et al.*, "Double-pass acousto-optic modulator system," Rev. Sci. Instrum. **76**, 063112 (2005).
15. I. A. Sulai and P. Mueller, "Laser spectroscopy of metastable palladium at 340 and 363 nm," Phys. Rev. A **102**, 042805 (2020).
16. A. Kramida, Y. Ralchenko, J. Reader, *et al.*, "NIST Atomic Spectra Database (ver. 5.11)," National Institute of Standards and Technology, 2023 [2024, February 3], https://physics.nist.gov/asd.
17. E. A. D. Hartog, M. E. Wickliffe, and J. E. Lawler, "Radiative lifetimes of Eu I, II, and III and transition probabilities of Eu I," Astrophys. J. Supp. Ser. **141**, 255 (2002).
18. J. Tenenbaum, E. Miron, S. Lavi, *et al.*, "Velocity changing collisions in saturation absorption of U," J. Phys. B **16**, 4543–4553 (1983).
19. S. E. Park, H. S. Lee, T. Y. Kwon, *et al.*, "Dispersion-like signals in velocity-selective saturated-absorption spectroscopy," Opt. Commun. **192**, 49–55 (2001).
20. A. Banerjee and V. Natarajan, "Saturated-absorption spectroscopy: eliminating crossover resonances by use of copropagating beams," Opt. Lett. **28**, 1912–1914 (2003).